IAC-21-A3.4B.4.x67075

ARGO: a planetary defense mission to test gravity traction techniques

Alessio Bocci[a]*, Lorenzo Ambrosi[b], Kevin Charls[c], Marco Gonella[d], Paolo Arighi[e], Alessandro Guerra[f], Nabil Iben Sobih Vazquez[g], Rashika Sugganahalli NB[h], Giorgio Taiano[i], Andrea Capannolo[j], Jacopo Prinetto[k], Michèle Lavagna[l]

[a] *Department of Aerospace Science and Technology, Politecnico di Milano, Via La Masa 34, 2016 Milano, Italy, alessio.bocci@mail.polimi.it*
[b] *Department of Aerospace Science and Technology, Politecnico di Milano, Via La Masa 34, 2016 Milano, Italy, lorenzo.ambrosi@mail.polimi.it*
[c] *Department of Aerospace Science and Technology, Politecnico di Milano, Via La Masa 34, 2016 Milano, Italy, kevincharls@mail.polimi.it*
[d] *Department of Aerospace Science and Technology, Politecnico di Milano, Via La Masa 34, 2016 Milano, Italy, marco2.gonella@mail.polimi.it*
[e] *Department of Aerospace Science and Technology, Politecnico di Milano, Via La Masa 34, 2016 Milano, Italy, paolo.arighi@mail.polimi.it*
[f] *Department of Aerospace Science and Technology, Politecnico di Milano, Via La Masa 34, 2016 Milano, Italy alessandro3.guerra@mail.polimi.it*
[g] *Department of Aerospace Science and Technology, Politecnico di Milano, Via La Masa 34, 2016 Milano, Italy, nabil.ibensobih@mail.polimi.it*
[h] *Department of Aerospace Science and Technology, Politecnico di Milano, Via La Masa 34, 2016 Milano, Italy, rashikasugganahalli@mail.polimi.it*
[i] *Department of Aerospace Science and Technology, Politecnico di Milano, Via La Masa 34, 2016 Milano, Italy giorgio.taiano@mail.polimi.it*
[j] *Department of Aerospace Science and Technology, Politecnico di Milano, Via La Masa 34, 2016 Milano, Italy, andrea.capannolo@polimi.it*
[k] *Department of Aerospace Science and Technology, Politecnico di Milano, Via La Masa 34, 2016 Milano, Italy, jacopo.prinetto@polimi.it*
[l] *Department of Aerospace Science and Technology, Politecnico di Milano, Via La Masa 34, 2016 Milano, Italy, michelle.lavagna@polimi.it*
* Corresponding Author

Abstract

Asteroid Redirection with Gravity tractoring and Observation (ARGO) is a preliminary mission design in the framework of the planetary protection topics; the 162000 (1990 OS) binary Near-Earth Asteroid system is selected as well-suited training environment to assess the gravity tractor (GT) technique effectiveness for potential Earth impact hazard mitigation, here applied on the system secondary. As a secondary goal, the mission would also scientifically characterize the system. The transfer to 162000 follows a low thrust trajectory performed with a flight proven ion propulsion technology. Power requirements of the propulsion system and EPS limits drove the transfer trajectory design. During close-proximity operations, several observation phases are envisioned to safely and robustly characterize both primary body and moonlet of 162000 and to allow safe GT operations. The characterization aims to map gravitational harmonics, shape, and orbital characteristics of the binary system along with spectroscopic, thermal inertia and volatile studies. The similar orders of magnitude of the gravity field of 162000 and SRP perturbation become, along with the EPS, the primary challenges in mission design during this phase. Intrinsically stable orbits are chosen to limit the use of propellant for active control. Separate communication phases are envisioned, allowing the downlink of science data between each major phase for ground processing. The ARGO mission relies on a secondary CubeSat for further observation and navigation during the GT phase, which also acts as a relay to allow unobstructed communication with ground stations. After the characterization phase, a robust combined rendezvous/station-keeping GNC system is designed to perform the towing phase using electric thrusters. It also accounts for orbital perturbations and uncertainties, and coping with ADCS for the multiple pointing requirements involved during GT operations. A high-speed impact with the moonlet is proposed as the End-of-Life strategy for ARGO, allowing a preliminary insight and comparison with the kinetic impactor technology. According to simulations, ARGO can operate a 15 % change in semi-major axis of the moonlet's orbit over a three-year span, thereby demonstrating the GT technology within a reasonable time frame. Additionally, thanks to the system partial

scalability makes the gravity traction be counted among the possible alternatives for effective planetary defense actions against non-characterized hazardous objects. This paper details the mission design with subsystem specifications and key technologies used in ARGO, providing an insight into its feasibility and current limitations.

Keywords: Binary system, electric propulsion, gravity tractoring, low thrust transfer, near Earth asteroid, planetary protection.

Acronyms/Abbreviations

ADC: Analog to Digital Converter
ADCS: Attitude Determination and Control System
AOCS: Attitude & Orbit Control System
BER: Bit Error Rate
CH: Characterization
CoG: Centre Of Gravity
CR3BP: Circular Restricted 3 Body Problem
EOL: End Of Life
EPS: Electric Power System
ESO: Extended State Observer
FOW: Field Of View
GNC: Guidance Navigation and Control
GS: Ground Station
GT: Gravity Tractor
HGA: High Gain Antenna
IR: Infrared
ISL: Inter Satellite Link
ITU: International Telecommunication Union
LGA: Low Gain Antenna
LNA: Low Noise Amplifier
LT: Low Thrust
LVLH: Local Vertical Local Horizontal
MGA: Medium Gain Antenna
MIB: Minimum Impulse Bit
NAC: Narrow Angle Camera
OBDH: On-Board Data Handling
PDF: Probability Density Function
PPT: Power Point Tracking
PPU: Power Processing Unit
RAM: Random Access Memory
RDV: Rendezvous
RF: Radio Frequency
SA: Solar Array
SES: Sun Earth Spacecraft
SRP: Solar Radiation Pressure
SS: Secondary System
SSTO: Self Stabilizing Terminator Orbit
std: standard deviation
TCS: Thermal Control System
TID: Total Ionization Dose
TMTC: Telemetry and Telecommand
UHF: Ultra High Frequency
WAC: Wide Angle Camera

1. Introduction

Potential Hazardous Asteroids (PHA) are asteroids which have relatively high probability of impacting the Earth compared to that in Kuiper belts. PHA are class of asteroids which stay near the Earth orbit, thus they are also called Near Earth Asteroids (NEA). Many mitigation strategies have been conceptualized in the past to deflect asteroid from impacting the Earth. Deflection techniques, such as kinematic impactor and nuclear detonation, essentially deal with instantaneous energy impartation to the asteroid as a way to deflect it. Whereas, techniques such as gravity traction and space tug use the mutual gravity field and the tugging force respectively for deflection. For this reason they require a large amount of time. In this study, gravity traction technique's feasibility is analyzed in the context of a real mission scenario. This report will delineate the feasibility study on gravity traction deflection technique. In the following sections, a brief description of the subsystems is presented.

2. Mission analysis

2.1 Interplanetary transfer

Initially a high-thrust transfer with a single gravity assist was computed. However, this resulted in a required burning time beyond the capability of any currently available deep space high-thrust propulsion unit. Thus, a low thrust alternative was investigated. The analysis was performed by using the Conway shaped-based algorithm [1] and then by optimizing it in order to obtain the minimum value of both ΔV and the thrust required. Moreover, taking this result as initial guess, a direct transcription method was implemented to get a bang-bang control law for the thrust profile. Without direct transcription, the maximum thrust required was 0.45 N, which exceeded the maximum thrust that can be extracted from the thrusters and the electric power available. As a consequence, the direct transcription method is here implemented in order to fulfil the constraints coming from EPS and propulsion subsystem. The direct transcription is set such that the maximum thrust available T_{max} is 0.29 N, moreover a maximum thrust profile depending on the distance from the Sun and available power is imposed as an upper limit for the transfer simulation. The equation describing the maximum thrust behaviour is directly taken, by

interpolation, from the engine performances. Moreover, another path constraint is added such that, when the spacecraft is far 2 AU from the Sun, the engines are powered off, relaxing the power demand.
The direct transcription uses 100 collocation points and as initial guess the result coming from the multi-objective optimization with the shaped based Conway algorithm.

Table 1. Parameters of low thrust transfer trajectory

Parameter	Value
Departure date	17/09/2027
Arrival date	20/11/2029
C_3	38.1874 km^2/s^2
α*	-0.1944 rad
β*	0.1680 rad
ΔV	3.67 km/s
T_{max}	0.29 N
M @ rendezvous	1859 kg

* α and β are the two angles in LVLH frame defining the orientation spacecraft injection velocity.

The aim of such an optimization is to further reduce the mass of propellant needed for the transfer and to limit the value of the thrust by a bang-bang control law. The final results are reported in Table 1, while Fig. 2 and Fig. 3 provide the thrust profile in mission time and distance from the Sun respectively. Finally, Fig. 4 reports the computed trajectory.

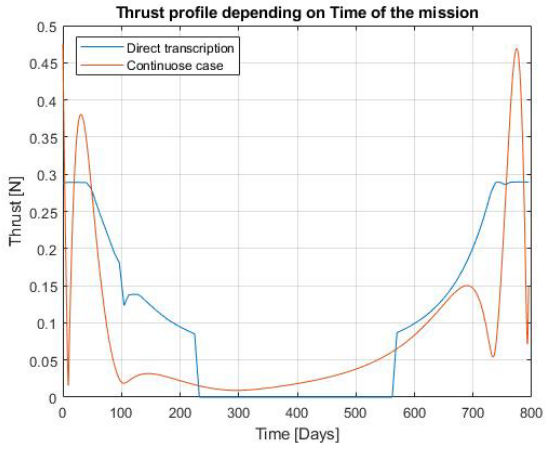

Fig. 2. Thrust required versus transfer time

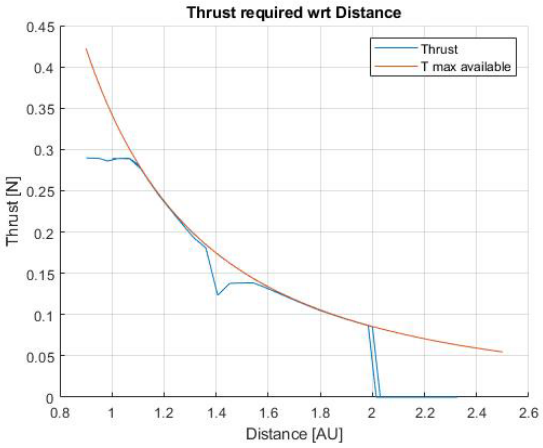

Fig. 3. Thrust required versus distance from the Sun

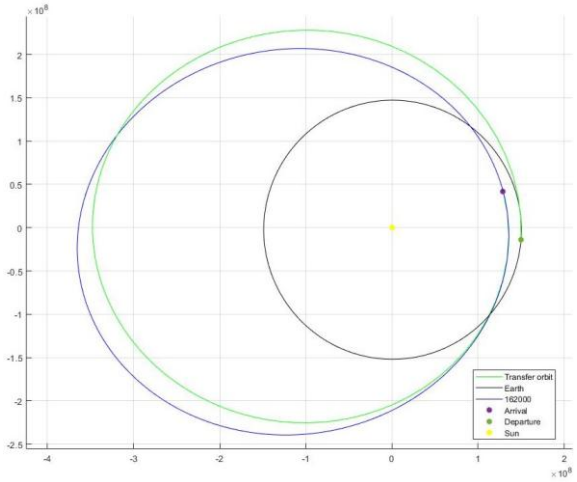

Fig. 4. Interplanetary transfer trajectory

2.2 Characterization phases

To compute the proximity trajectories and operations, the following assumptions are made:

1. The moon-let orbits are around the primary with an eccentricity of 0.1. Their plane is co-incident with the heliocentric orbital plane.
2. Both primary asteroid and its moon-let spin with their axis perpendicular to the heliocentric plane.
3. The moon-let is tidally locked with the primary asteroid, thereby defining its spin rate.

The initial properties of the binary system and their uncertainties can be estimated from ground-based observational data and through literature survey [2]. This level of uncertainty at arrival from interplanetary transfer, besides general science objectives, forces a detailed multi-step characterization phase to study the binary system. The final expected parameters and

uncertainties can be estimated basing on the on-board imaging instrumentation resolution and through Monte Carlo simulations. Results are reported in Table 2.

Table 2. Initial and final estimated properties of binary system during characterization phase

	Initial parameters		Final parameters	
	μ (mean)	σ (std)	μ (mean)	σ (std)
ρ [g/cm^3]	1.60	±0.08	1.60	±0.02
d_p [m]	300	±20	300	±1
m_p [kg]	2.29e10	±4.70e9	2.26e10	±3.61e8
d_s [m]	50	±20	50	±1
m_s [kg]	1.55e08	±1.64e8	1.05e8	±6.43e6
a_s [km]	0.6	±0.03	0.6	±0.008
e_s	0.0	+0.1	0.0	+0.1

* ρ= density, d=diameter, m=mass, a= semi-major axis, e=eccentricity, p=primary, s=secondary

The spacecraft arrives at the perihelion of the binary systems orbit after the interplanetary transfer. But, for initial characterization, considering the rate of variation of lighting conditions, the solar flux for SRP and the slow relative variation of spacecraft's position with respect to the binary, the aphelion is more optimal. Thus, a relative rendezvous formation trajectory is computed to transfer ARGO from perihelion to aphelion.
The dimension of this bounded orbit is defined to allow at least 100 m/px imaging resolution at aphelion for guidance to more proximal orbits. The final orbit in LVLH frame is reported in Fig. 5, with closest approach distance of 1000 km. The orbit is computed using a Michael Tillerson relative orbital dynamics model for eccentric orbits [3].

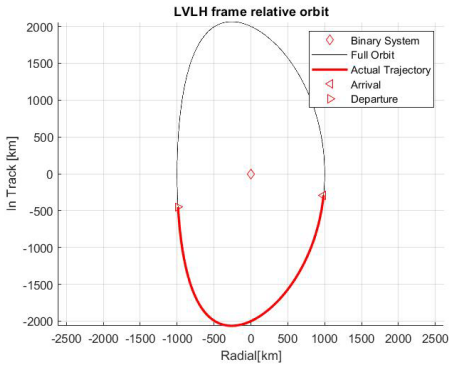

Fig. 5. Relative rendezvous formation trajectory

In order to perform the initial characterization phase, at aphelion, a closer bounded orbit is defined in the LVLH frame. The goal is to image both asteroids with an imaging resolution of 1 m/px with 10 imaging passes on the surface. The designed orbit has a closest approach distance of 10 km as shown in Fig. 6, with a total imaging time of 9.35 days. Additionally, a standby communication time-period of 2 weeks is allotted between any major phases, bringing the total time spent in the trajectory to 37 days.

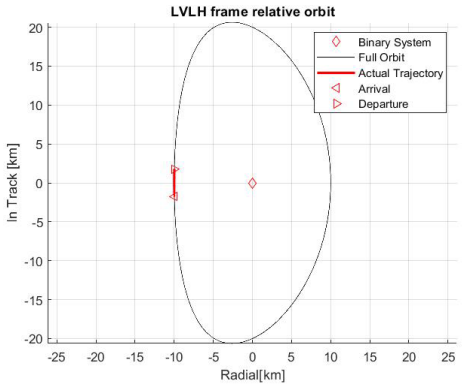

Fig. 6. Initial characterization orbit

After the initial characterization, the on-board models of both objects are updated, allowing closer refined orbits in the binary system. To provide safe-hold standby point and to perform imaging and thermal studies around the terminator plane, an SSTO is computed. This is a bounded orbit which can be defined around low-gravity objects where SRP perturbations are significant. The full development of an SSTO is explained in detail by D. Scheeres in [4]. The final size of the orbit (see Fig. 7) is defined by considering the condition at perihelion, since SRP is strongest at this point. The orbit selected has a semi-major axis of 1.6 km and a Λ parameter of 85.83° with a down pointing eccentricity vector. The robustness of the orbit was studied considering a ±10 % variation in area to mass ratio and the uncertainties of the binary expected at this phase.

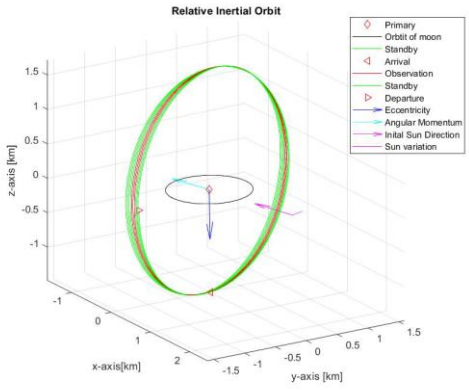

Fig. 7. Self-stabilizing terminator orbit

To better refine the shape and gravitational models of the system, a main characterization orbit was developed. The specific orbit designed is a polar eccentric orbit, with apoapsis of 3.5 km towards the Sun direction. This orbit is sized to provide an imaging resolution of 35

m/px on the primary body. The goal is to obtain visual imaging at apoapsis and thermal imaging of the two bodies at periapsis after ARGO crosses the terminator plane. The orbit is developed considering the circular restricted three-body problem assumptions and the results are given in Fig. 8. The choice of the polar orbit was driven by the need to reduce the 3rd body effects and to provide an off-orbital plane mapping of the system.

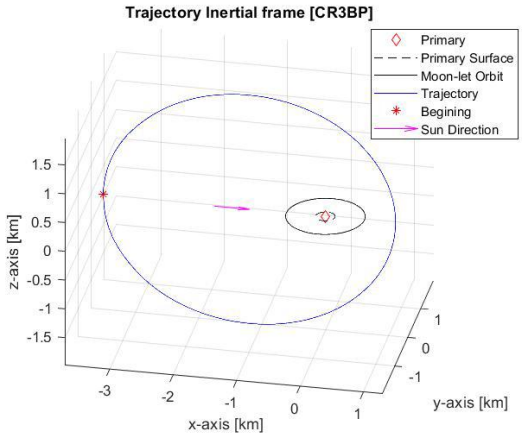

Fig. 8. Main characterization orbit

After the main characterization phase, ARGO returns to the SSTO orbit, for communication of results and updating of the on-board models. Before proceeding with gravity tractoring, ARGO deploys IASON, the secondary segment, into its own SSTO orbit for observation and communication during GT operation. Since the area to mass ratio of IASON is 0.0275, the final required semi-major axis of the SSTO is 1.35 km. The transfer trajectory for IASON from the original SSTO to its orbit is reported in Fig. 9. The total transfer takes 2.2 days with a ΔV of 0.51 cm/s. The initial impulse for transfer is provided by the spring deployment mechanism, while the rest is provided by on-board mono-propellant propulsion.

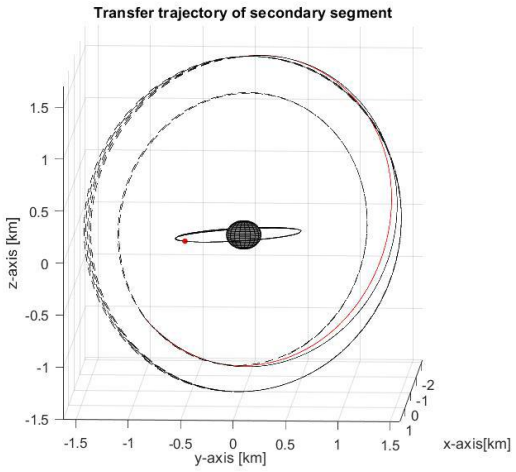

Fig. 9. IASON transfer trajectory to observational orbit

Once IASON is deployed, the main segment ARGO proceeds to a circular orbit around the primary to validate the orbital models and perform further particle science on the binary. This orbit will also be used as second standby point for further operations in the binary system. To compute the orbit, a two-body solution is differentially corrected to produce an orbit in a CR3BP, which is then further corrected to include the spherical harmonics of the primary body. The orbit is chosen basing on the final parameters and uncertainties expected displayed in Table 2, resulting in an orbital radius of 0.299 km. The sizing was selected to reduce the 3rd body influence of the moon-let, still being at a safe distance from the primary asteroid. The final results are shown in Fig. 10.

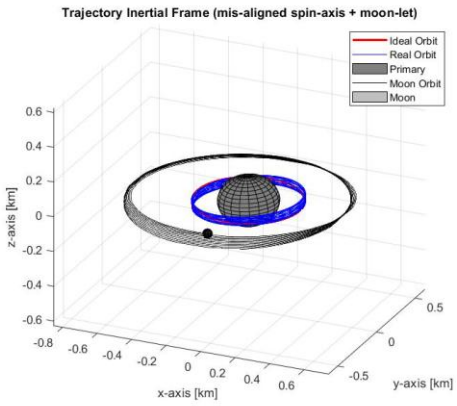

Fig. 10. Circular orbit around primary

Once all on-board models are validated, a free return trajectory is used to transfer ARGO from a circular orbit around the primary to moon-let's proximity. The free return trajectory was chosen to allow an easier abort in the case of emergency. Indeed, without burn at the moon-let, the spacecraft naturally returns back to the

primary asteroid, thanks to this particular type of trajectory. The specific method to develop such a trajectory is explained extensively by Jesick [5]. The method involves a two-body problem guess solution to develop an initial solution in CR3BP, which is then used to estimate the final orbit through a single parameter continuation. The orbit is sized basing on the minimum distance expected at flyby at the moon-let during transfer. This value was selected equal to 0.158 km. The development of the trajectory in CR3BP synodic frame with all the families found during continuation is shown in Fig. 11.

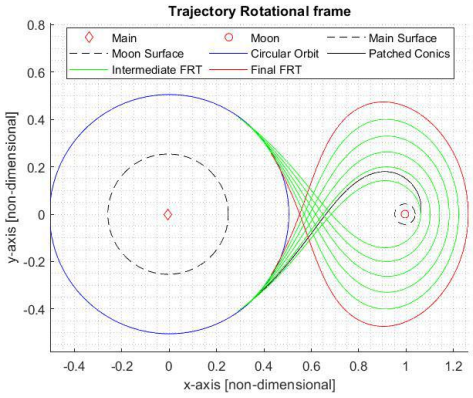

Fig. 11. Free return trajectory in synodic frame

The final trajectory in the real system is computed with differential correction, including the orientation of all bodies, the spherical harmonics and ellipticity of the moon-lets orbit. Fig. 12 presents the trajectory.

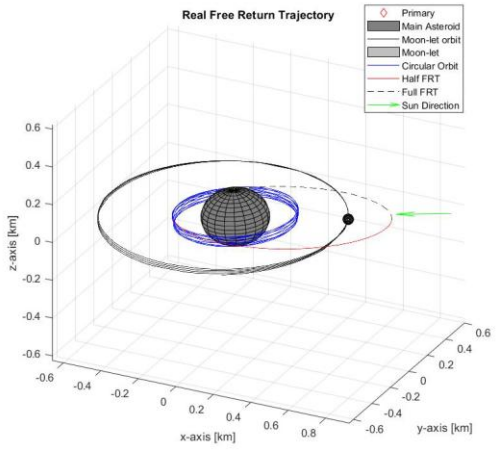

Fig. 12. Free return trajectory in inertial frame

Before performing the GT operation, a full free return trajectory orbit is performed to rehearse the transfer, image the moon-let closer and perform final check out of all systems. Then, ARGO returns back to the circular orbit before performing the actual transfer to the desired location near the moon-let. At the end of this transfer, the specific guidance controller developed in the GNC section brings ARGO into the correct position to perform the GT operation.

The full characterization phase, including all the transfer trajectory, requires 1.06 m/s of ΔV and lasts 495.5 days. A further 5.58±1.22 m/s is required for all the station keeping, bringing the overall ΔV budget to 7.87 m/s. This result is within the 15 m/s of propulsion budget allotted to this phase of the mission, with enough margins for robustness and safety. For further safety during GT operation, possible emergency abort trajectories to SSTO orbit were analysed. This resulted in a reserved budget of 3 m/s to perform up to 10 such aborts during all phases of GT operation.

2.3 End of life

At the end of the GT operation, the EOL strategy adopted for the main segment is to impact the moon-let, allowing possible investigation of the kinetic impactor method for asteroid deflection. The particular strategy developed involves coasting 871000 km from the binary towards the Sun direction and performing a continuous burn till impacting the moon-let, achieving an impact velocity above 500 m/s. The scheme of this strategy is reported in Fig. 13. The impact and its overall effect will be observed by IASON segment. To protect the IASON segment, the impact is timed such that IASON is at the far side of its SSTO orbit, away from the impact location. The total expected ΔV for EOL is 558 m/s which is mostly provided by the low thrust propulsion system using 20 kg xenon propellant.

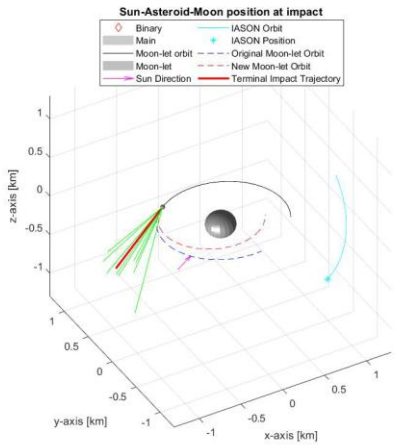

Fig. 13. End of life of ARGO segment

3. GNC

In a similar fashion to what is done in [6], an hovering canted thrusters tractor is selected. It is oriented on the

velocity vector of the moonlet in order to maximize the effectiveness of the traction.
The spacecraft shall perform an initial RDV from the previous characterization orbit to the desired GT position; once achieved, station keeping will hold it using electric thrusters operated by the control system.
The main goal is to design a control system capable of satisfying these requirements both in terms of effectiveness and robustness with respect to perturbations acting on the system and uncertainties on some critical values.

3.1 Model assumptions

The assumptions made to perform the design are:

- The primary asteroid and its moonlet are considered in the ideal case as perfect spheres of radius R_1 and R_2 and masses m_1 and m_2 respectively, while in the non-ideal case as two oblate spheroids of ellipticity ϵ_1 and ϵ_2
- The spacecraft is considered as a point of mass m_3
- The system is modelled as a three-body problem
- The perturbations acting on the system are the SRP and the spheroidal effects of the gravitational fields modelled by the spherical harmonics $(J_1, J_2, \dots, J_n)$
- The spacecraft is subjected to the thrust provided by the engines (namely the control force)

The control system is supposed to compensate the external forces and inertial contributions but not the perturbative forces since, in general, they are not known a priori. The robustness analysis will verify that even against disturbances the control system is effective.
In order to maintain the desired position aligned with the velocity of the secondary asteroid with zero relative velocity, a non-linear control system based on the results of asymptotic stability of the Lyapunov function is adopted. The desired position and velocity are imposed by means of quadratic forms and the parameters of the control system are suitably tuned (a similar control law was obtained by [7]).
In order to take into account the excessive proximity of the spacecraft to the surface of the secondary asteroid, a further contribution within the control law to grant collision avoidance is introduced by defining the gradient of an artificial repulsive potential (see [8]).

3.2 Simulation and results

A Monte Carlo simulation is performed with 20,000 randomatic couplings with an integration step of 15 minutes over the three years. The effective total mission time is evaluated afterwards once the goal of 100 meters variation of moon's orbit semi-major axis is achieved.
Main parameters (radius, ellipticity and mass) nominal values and uncertainties are reported in Table 2, while for perturbing initial conditions we considered:

- a not negligible but bounded error in position with respect to the mission analysis predictions
- an excess or defect of velocity at the RDV starting point with respect to the mission analysis predictions

The parameters under investigation are: the maximum thrust required to perform RDV and GT phases, the total amount of time needed for RDV and GT phases, the semi-major axis variation of the moonlet and, finally, the maximum position error during GT phase. Results are satisfactory and present the same behaviour.

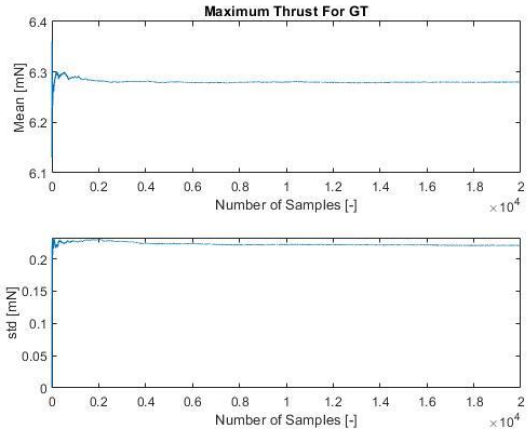

Fig. 14. Monte Carlo analysis: thrust for GT

In Fig. 14 the progressive convergence of mean and standard deviation are presented for the maximum thrust required during the GT phase.

Table 3. Monte Carlo analysis main results

	RDV		GT	
	Min.	Max.	Min.	Max.
Thrust [mN]	21.4	75.5	5.75	6.85
Time [d/y*]	1.09 d	1.19 d	2.39 y	2.79 y
Δa [m]**	-	-	100.0	100.2
Err. [m]***	-	-	5.04	6.65

* d=days, y=years
** Δa= moon-let semi-major axis variation
*** Err.=Position Error

Table 3 summarizes the upper and lower bounds value for the studied performances on both phases.
The higher thrust requirements are at the beginning of the RDV manoeuvre since the spacecraft is accelerating

coming from an outer orbit. In the case of the RDV the time required resembles to the moonlet orbital period while for in the GT manoeuvre it is lower than the maximum allowed value of three years.

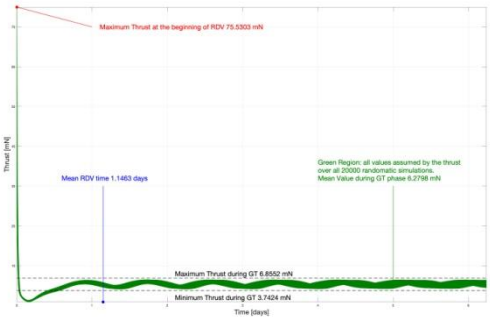

Fig. 15. Overall thrust profile

Fig. 15 presents the superposition of all thrust curves in the range of the first 6 days of the mission. After the initial transient of the RDV (from initial condition to desired position to start GT) the thrust stabilizes its behaviour oscillating in the bounded region 3.74-6.86 mN. The oscillation frequency is of the order of days for lower times and for higher of the order of hours; this makes the actuation possible by available thrusters technologies.

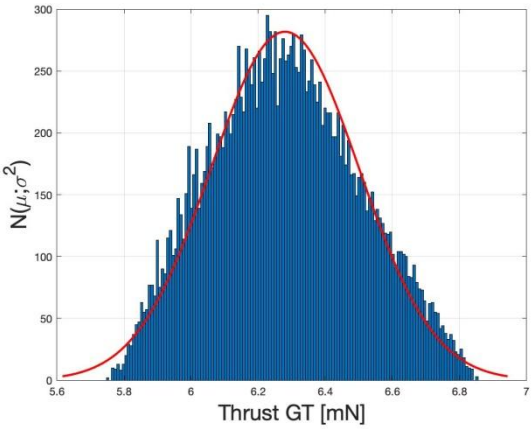

Fig. 16. GT thrust distribution

Since the perturbations (gravitational in particular) acting on the system are strongly affected by binary system properties, it is expected that changing in a randomatic way the inputs, but with a Gaussian PDF, then the system responds in a such similar Gaussian way. Once Monte Carlo analysis is performed and mean and standard deviation are evaluated, it is possible to build backward the PDF; this concept is graphically presented in Fig.16.

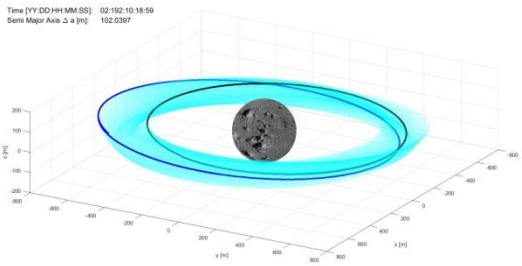

Fig. 17. Orbit evolution during GT

Finally in Fig. 17 the overall moon orbit evolution is presented.

4. ADCS

ADCS shall perform efficiently the detumbling, slew and tracking manoeuvres with requirements for pointing in multiple directions. Table 4 shows the several required configurations along the mission and Table 5 the associated pointing errors for the space segments:

Table 4. Required directions

	Directions set 1	Directions set 2
ARGO	Thrust and Sun (interplanetary transfer phase)	Thrust and binary system (GT phase)
IASON	Sun and binary system (observation mode)	Earth and binary system (telecom mode)

Table 5. Pointing error

	Directions set 1		Directions set 2	
	TMTC	Sun Direction	Thrust Direction	Cameras
Pointing Error	0.1°	5°	0.025°	0.01°

It follows the selection of Star Trackers as primarily attitude determination sensors because of high level pointing requirements. While Sun sensors account for Sun position. Instead, for IASON to correct re-point the spacecraft from telecommunication to observation mode. To study the control needed to satisfy pointing requirements, the focus is on operations during the GT phase, because of the higher number of constraints.

4.1 Model simulations and analysis of the results

Several rotational dynamics simulations have been performed for both ARGO and IASON, implementing Euler equations for rotational dynamics in the presence of SRP and gravity gradient disturbances. Attitude kinematics is investigated using quaternions, adding a

proper ESO based on Kalman filter to cope with estimation errors (see [9]).
To be operatively fast and according to the inertia involved, the following configurations are selected:

- twelve monopropellant thrusters for ARGO (they can also provide thrust for any corrective impulsive manoeuvres during GT).
- double four cold gas thrusters to save mass and provide redundancy for IASON

To avoid chattering, all control laws based on sliding-mode are combined with the Schmidt trigger logic with in addition, for the secondary segment, a fast pseudo inverse approach to control allocation with ADC adopted for the optimal thrusters selection.

4.1.1 Detumbling phase

The bang-bang control law is used starting from a high initial angular velocity 5°/s - 10°/s, due to spacecraft release from launcher for ARGO and the deploying mechanism for IASON. The angular velocity, after a short transient, eventually reaches the asymptotically non-zero value due to background disturbances and the non perfect on/off behaviour due to characteristic MIB and rise time of the thrusters. It results a faster response of the ARGO with respect to IASON because of the more efficient thrusters configuration as well as the higher nominal torque.

4.1.2 Slew phase

The classical nonlinear control plus a *bang-bang* like one is applied with the gains optimally tuned. The ARGO dynamics is faster than the other, but designed to grant the proper agility during the characterization orbits for fast antenna re-pointing. The angular velocity is always below 5°/s in order to avoid structural issues of flexible appendages.

4.1.3 Tracking phase

Tracking is the most important ADCS task for both the segments; it shall grant high precision during firing of thrusters in the heliocentric transfer and, during the GT, the desired attitude to ARGO. Moreover IASON needs the correct orientation for imaging the binary system. In order to deal with more than two years of mission with continuous tracking, 4 reaction wheels in pyramidal configuration are used. This choice accounts for redundancies and to minimize the desaturation problem (specially for ARGO). The same electric thrusters used for GT (that can be canted thanks to the 2 gimbals DOF) are adopted to provide the desaturation torque. For IASON, reaction wheels desaturation is less stringent and the same thrusters adopted for detumbling and slew are used. To properly size the systems a typical nonlinear control for reaction wheels is implemented with an additional control by thrusters to compensate the wheels deceleration and the tumble induced by torque mismatch. For ARGO the system is initially able to provide the 0.1° pointing requirement of TMTC and then it reaches the required 0.01° of the navigation cameras. In the same way IASON achieves the required 0.01° pointing error for imaging cameras and the 5° one in the Sun direction.

5. Propulsion subsystem

Avoidance of plume impingement of the surface of the asteroid is a mandatory requirement for the system, as the resulting force would nullify the tractoring effect. Engines with well-defined plume behaviour and narrow divergence angles are thus required to perform this operation.
This unique requirement and the long duration of the gravity tractoring lead to the selection of gridded ion thrusters for this phase of the mission.
The wide gap between the thrust class required by gravity tractoring and that of an eventual interplanetary low-thrust transfer, however, does not allow a single set of engines to perform both operations.
Nonetheless, having ion thrusters on board represents an opportunity for a low-thrust transfer design, as propellant tanks and part of the feeding lines could be shared by both gravity tractoring and transfer branches, reducing overall mass and complexity of the system.
Comparing these considerations with results from mission analysis leads to the selection of a low-thrust interplanetary transfer, performed by a solar electric propulsion system. Advantages of this choice include a simpler tanks layout, a lower volume of the system and fine trajectory control thanks to the high thrust accuracy of the engines.
The set of thrusters performing the interplanetary transfer are supported by power supplies and flow control units operating according to the highly efficient bang-bang control logic, while gravity tractoring engines are finely tuned in time to the specific requirements of the manoeuvre by their relative support devices. Flight-proven components are preferred for the mission, but the subsystem is nonetheless designed to be fully redundant.
To guarantee the high responsiveness required by the ADCS, a secondary monopropellant-based propulsion subsystem is also envisioned. Thanks to compatible pointing mechanisms, electric thrusters can nonetheless support ADCS operations.
Moreover, as solar panels are pivoted away from the Sun during the characterization phase in order to mitigate SRP disturbances, a trade-off between electric

power availability, orbital stability and Δv requirements is performed, leading to the allocation of this phase to the chemical subsystem.
EOL operations are jointly performed by both subsystems.
Regarding IASON, stringent mass and volume constraints direct the design to a single chemical propulsion subsystem. A set of highly versatile all-in-one engines is selected, each combining a main monopropellant-based thruster for translational manoeuvres and multiple cold gas ones for attitude control.

6. EPS

For ARGO mission, one of the main advantages is that the distance of the SA power-run is always lower than 3 AU from the Sun as we are targeting a Near Earth Asteroid system. After a trade-off, SA emerged as a successful competitor for the common operations to be conducted in our mission. A power of 9 kW will be required during the LT transfer, which implies 80% of the power demand. For a continuous GT phase the average power demand reduces to 1.5 kW. For the sizing and configuration during the rest of the phases we considered as one of the main drivers the area to mass ratio for SRP stability issues in the binary system's environment.
The profile of the thrust has been designed in a *bang - bang* thrust constrained to be under the curve of power availability during orbit. The efficiency of the solar cells diminishes with lower irradiance and with increasing temperature. Furthermore, the further from the Sun the more demanding the TCS becomes. Thus, we imposed to cut off the thrust further than 2 AU where the solar irradiance is around 360 W/m^2.
Since the orbit is very eccentric and will suffer from wide variations of the IV curve, we selected the fully regulated bus with PPT architecture for the power control of the main spacecraft. Moreover this strategy avoids thermal dissipation problems with the high current and power needed. The configurations of ARGO and IASON can be found in Table 6 and Table 7 respectively. The components of ARGO are shown in Fig. 18. IASON will incorporate a similar configuration just using one PPU and a standard bus of 28 V.
Concerning the configuration of the panels, the constraints are driven by the tracking and canting methodology, as well as by the interference with possible AOCS propulsion and instruments placed on the sides of the spacecraft. Two arrays will be placed coplanar to the Sun direction vector granting a symmetric shape at the moment of canting the solar panels near perihelion, not just to lower the power harvested but to control the SRP perturbance.

Table 6. ARGO EPS specifications

	ARGO PV	IASON PV
Driver	Perihelion – Transfer	Aphelion – GT
Voltage/Current	103/139 [V]	29.8/4.77 [A]
Area [m^2]/Conf.	34.4/31s301p	2.47/8s85p
Array / Module	2/3	4/3 shuttlecock 10°
Mass [kg] / Mar. Mass [kg]	262/314	33/40

Table 7. IASON EPS specifications

	ARGO BAT	IASON BAT
Driver	3.6 h eclipse –GT	50 min eclipse – assessment
Voltage [V]	28	28
Capacity [Wh] / Configuration	182/8s8p	182/8s1p
Cycles/DOD [%]	<3000/70	~ /80

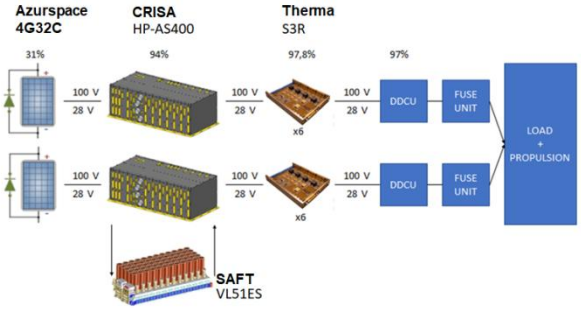

Fig. 18. Main spacecraft EPS architecture

7. TMTC

The TMTC subsystem provides essential communication to and from the spacecraft. In this section definitive communication ways for ARGO and IASON segments are drafted. Link characterization and solutions for efficient communication with Ground segments are also reported.
The main requirements from the telecommunication systems are the link availability and the reliability of the received data. To guarantee these conditions the system is sized considering the interfaces with ADCS, EPS, OBDH and Structure/Thermal. Highlights of the tasks to be performed throughout the mission includes:

- telemetry and telecommand throughout the mission.
- scientific data return from ARGO segment after first and subsequent characterizations and analysis of the data to update the gravity model onboard.

- telemetry from IASON segment during GT operations and telecommand, if any. IASON acts as relay between ARGO segment and Earth's ground segment.

Use of radio frequency spectrum is regulated by the international treaty (ITU). X-band frequencies being below 10 GHz can be considered as it will be more resistant for both telemetry and telecommand using MGA. To support the huge amount of data transfer during the science phases, parabolic HGA is commanded to operate in Ka band. As the IASON segment will be deployed after the characterization phase 2, ARGO and IASON segments operate in closer proximity with maximum distance up to 5 km. Hence, it is straight for us to choose UHF band (450 / 432 MHz as forward and return link respectively) discarding the option of X or Ka band for ISL which requests high RF power.
For the reliability of the information the system shall guarantee a BER of 10^{-7} for the telemetry transmission in the downlink and for the command from the ground. It shall also guarantee a BER of 10^{-5} for the downlink of the scientific data. Telecommunication modes along with the data rates for each phase is depicted in Table 8.

Table 8. Telecommunication modes

Phases	ARGO/ IASON	Data Rate (bps)	Data Volume
Pre Launch	Off/Off	-	-
Launch	Off/Off	-	-
Interpl. Leg*	On/Off	>800	Low
CH1	On/Off	$>1.5\times 10^5$	Very High
IASON depl.**	On/On	$>5\times 10^3$	Medium
GT operation	On/On	$>1.5\times 10^3$	Low
Disposal	On/On	>500	Low

*Interpl.=Interplanetary
**depl.=deployment

The antenna gain parameters are extracted from the data manual directly. All the necessary calculations are done considering the worst case distance between both radios when the ARGO and IASON are on the horizon of the ground stations. Deep Space Antennas located in Australia, Spain and Argentina are utilized for ground link to have access for the larger communication window. The misalignment losses were evaluated considering a pointing accuracy of 0.1° and it is verified that the ADCS system satisfies the pointing accuracy requirement.
During the Interplanetary transfer ARGO system is hidden twice, highest being for a period of 27 days from 360th day and then 7 days after approximately 600 days after launch. ARGO system is out of communication window due to the Sun for 11 days before starting CH phases. During these periods, when SES angle is below 3°, complete communication will be shutdown and recovery of the same will happen at low data rate when SES angle is between 3° and 7°. During CH 3 and GT periodic obscuration of ARGO segment is due to asteroid bodies. However IASON is able to communicate with the ground segment.
The mass and power estimation for this subsystem is mainly derived from the manufacturers handbook. The mass of the parabolic reflector HGA is defined as $m = K_p A$ where A is the physical area of the HGA. The proportionality constant K_p is assumed to be 6, this is derived from [10]. The margin considered is 5% for the mass estimation as the lines cannot be defined definitively at this moment while a 20% margin is applied on the power consumption due to the higher uncertainties on the filters, LNA and oscillators.

8. OBDH

ARGO Mission involves conducting characterization and long duration proximity operation as part of mission requirement, this demands high processing and data storage from OBDH subsystem. In the following section, ARGO mission's OBDH subsystem design is presented. Once the strategy of the communication is fixed by the TMTC subsystem, calculation of the data storage is accomplished by analyzing the payload data acquisition strategy. To properly size the data storage, imaging strategy is adopted which will give the approximate number of images acquired per day. During Characterization phase, the aim is to fully image both primary and secondary asteroid. Assuming the spacecraft sufficiently far away from the binary system, the angular size of the asteroid bodies will fit inside the field of view of imaging instruments. The implemented plan to acquire 5 sets and 1 set of images for primary and moon-let respectively are devised to enhance the availability of more images for science and also to be complaint with transmission capability of TMTC.
To meet the requirements of the ARGO segment, processor sizing is carried out for modules:

1. *Service module processing unit* which takes care of the platform related to the processing requirement. The design point for the sizing is considered to be the GT phase. It has a total throughput of 40.882 MIPS and 75.185 Mbits of RAM.

2. *Payload module processing unit* takes care of the processing of the instruments data. Along with data processing and compression requirements, ARGO segment is required to do vision based navigation for autonomous relative navigation. The sizing is done for worst case scenario where the total

throughput and memory sum up to 246.84 MIPS and 139.4 Mbits respectively with 400 % margin.

The bus selection is preceded by the estimation of the data rates of the individual subsystems and of the onboard instruments. In a similar fashion, by analyzing the data rates of each individual subsystem/instrument, suitable buses are selected. After having selected the buses, integration of all the sub components of the OBDH is carried out to form hardware architecture. Service and payload modules are to be connected by Mil-STD-1553B bus. During the components selection, redundancy strategies are tailored so that the system is fault tolerant and includes 2-point failure architecture. This makes the system robust and reliable to cope with higher processing and data handling support required for the mission. For both service and payload module, processor units work independently without sharing the workload. Two processors are in hot redundancy (to provide software redundancy) and two are in cold redundancy.
Concerning the IASON segment, the processing demand is relatively low compared to Argo segment. As a result, selection of single processing unit is preferred. Thus, the central processing unit configuration is adopted to handle both subsystems and the instruments.
Components selected for both ARGO and IASON will sufficiently satisfy the processing as well data storage requirement. Many of the components have their TID < 300 krad which is the standard requirement for components used in space missions.
From the research survey of SPENVIS, in order to have a TID resistance of 300 krad, a thickness of 5 to 6 mm of Aluminium slab is required. Based on this, the shielding box is sized. The mass of the shielding box for ARGO and IASON segments are 9.49 kg and 3.35 kg respectively.

9. Structural design

The preliminary configuration proposed for ARGO and IASON is the result of an iterative procedure and not optimized in terms of volumes.
However, it is designed to satisfy the correct and simultaneous functioning of the various subsystems in the different mission phases.
Power production, instruments field of views and communication subsystem in the science and GT phases are the main drivers for the design.
Preservation of the centre of mass, thermal control and effectiveness of attitude control are also taken into account as secondary drivers. Indeed it is possible for them to adopt counteractions or accept lower performances.
The configuration is also constrained in size and mass distributions by the selected launcher [11].

9.1 ARGO design

The parallelepiped shape is preferred for simplicity and pointing requirements, since it is possible to mount the required instrument on the face pointing towards the target.
Moreover, this solution has been widely used in past missions to asteroids or comets, such as Dawn, Rosetta, OSIRIS-REx and the two Hayabusa.
Once the volume and position requirements of the various subsystems are known, the shape is chosen as a cube of 2 m side.
Mobile appendages, payloads and thrusters are allocated on the external surfaces according to the pointing and interference requirements.
Referring to Fig. 19, the electric propulsion subsystem takes the lower part of the spacecraft. Xenon tanks are placed inside the structural cylinder in order to preserve of the CoG alignment to minimize the loads during the launch.
Batteries and elements that require lower temperature are placed near the $-y$ face.
The 12 chemical thrusters position guarantees the authority with respect to all the three main axis of the spacecraft and also avoids interference between the plume and external appendages.
The arrangement of the 8 electric thrusters avoids interference between themselves and with the adapter chosen.

9.2 IASON design

Applying the same philosophy, IASON is designed as a cube of 0.60 m side. Each lateral face hosts a solar panel, while the thrusters and the HGA are placed on the two other faces.
Panels are characterized by a shuttlecock configuration. This allows to use cells of standard dimensions but at the same time to avoid the interference between panels and FOW cameras.

9.3 Structure

The structure of ARGO and IASON is sized to support static and dynamics loads in the most demanding condition, that is the launch.
The sizing load conditions refer to those provided by Ariane 6 User's Manual [11]. Then the structure is also validated in the case of launch via Ariane 5 [12].
A detailed analysis in terms of natural frequency requirements is also performed.
The primary structure of the two segments is made up of beams and sandwich panels. Aluminium alloy AA7075 is selected as primary material due to its stiffness and buckling resistance while aluminium honeycomb is chosen for the sandwich core.

The structure of ARGO and IASON is sized with an iterative process of design and verification, based on static analysis.
The structural analysis is performed by a FEM simulation, using Autodesk Inventor Nastran for both modelling and resolution. About 1300 kg of the current 1400 kg of non-structural masses are included in the model as concentrated masses, increased by a margin of 10%. The non-structural part of the mass excluded from the simulation is due to distributed elements such as cables and pipes.
The primary structure is designed as a load-bearing truss to which six panels are connected. A central cylinder (of the diameter of the spacecraft-adapter interface) is used to distribute the loads between the adapter and the central panel and to support the lower module, which houses the electric propulsion subsystem.
In the upper module, a central cone houses the hydrazine reservoir and supports on top IASON.
The same procedure is used to design IASON structure.
The results of static analysis are reported in Table 9:

Table 9. ARGO static analysis

Segment	ARGO	IASON
n° nodes	576,122	407,361
n° elements	306,321	208,874
d_{max} [mm]*	0.98	2.17
SF_{min}**	2.171	6.894
Str.*** mass [kg]	364.912	8.683

*d_{max}= maximum nodal displacement
** SF_{min} = minimum nodal Safety Factor
***Str.=Structural

Finally, a dynamic analysis is performed on the assembly of ARGO and IASON segments in the launch configuration to check launcher requirements.
Buckling analysis is also performed to verify that instability doesn't occur.

10. TCS

The goal of the TCS is to keep all the spacecraft components within their temperature limits throughout the whole mission's lifetime [10]. This preliminary design is the result of an iterative process which takes into account the thermal requirements, the interactions with other subsystems and the available technologies as main drivers. Moreover, considering the duration of the mission, the failure avoidance and risk minimization are also relevant drivers. For those reasons, the TCS focuses on passive control systems such as coatings together with heaters and shunt resistances.

10.1 Model and assumptions

To study the thermal properties of the systems, a 10 nodes analysis and a 7 nodes analysis are set for the ARGO main body and the IASON main body respectively. This is done to model all the on-board instruments and devices with different temperature ranges and optical properties. It is also assumed that all the nodes are exchanging heat with the others only via radiation.
Fig. 19 and Fig. 20 together with tables Table 10 and Table 11 show the nodes orientation and what each node represents. (node 10 is the internal node and it's not shown).

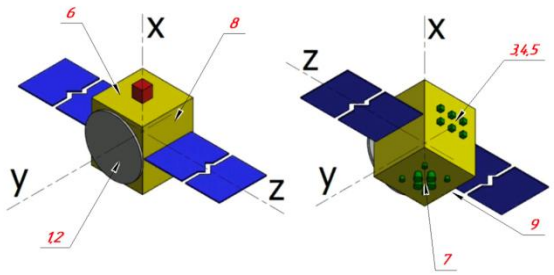

Fig. 19. 10 nodes orientation

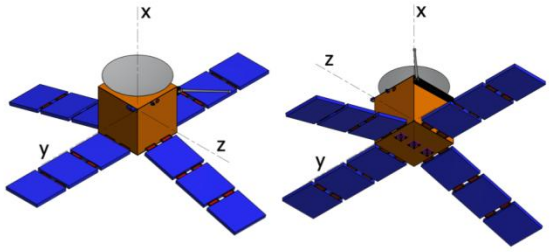

Fig. 20. 7 nodes orientation

Table 10. Node modelling for ARGO

Nodes	Surface / Equipment
1	LGA, Face 1
2	HGA, MGA
3	WAC, NAC, Thermal IR
4	Laser Altimeter
5	Face 2
6	SS, Face 3
7	Engines, Electronics
8	Solar Panel Face
9	Solar Panel Face
10	Tanks, Batteries

Table 11. Node modelling for IASON

Nodes Directions	Surface / Equipment
$+x$	HGA
$-x$	Engines, Electronics
$+z$	WAC
$+z$	Face 3
$-z$	Face 4
$+y$	Face 5
$-y$	Face 6

Concerning the solar panels, the solar cell used are of the QJ Solar Cell 4G322C – Advanced type provided by AZUR SPACE [13]. They are modelled as follows: the front surface absorptivity α_{front} and emissivity ϵ_{front} are considered to be equal to 0.64 and 0.8 respectively. This way, the ratio α/ϵ is equal to 0.8 which is a standard value for solar cells. The back of the surface emissivity ϵ_{back} is set to 0.7. This is obtainable by using grey paintings together with layers of aluminized Kapton [10]. Finally, the efficiency η_{sp} to convert solar irradiance into electricity is set to 0.32 by the cell type. By using these optical parameters, the solar panels are caplable of dissipating the high energy received from the Sun at perihelion and avoiding freezing temperatrue at aphelion.
During the simulation, the energy from the Sun can be considered the only external energy source, since both the Earth albedo and the Earth IR radiation can be considered negligible due to the larger distance from the Earth. However, while at 0.9 AU there is plenty of energy, at 2.4 AU the heat coming from the Sun drastically drops and heaters are required.
The simulations are performed considering steady-state conditions during all phases of the mission. The only exceptions are the GT phase and the eclipse phase. In those cases, a transient simulation for the worst case scenario using an Autodesk Inventor Nastran software is done.

10.2 Results

The final TCS design is the result of many iterations. Starting from the analysis of the worst hot and cold scenarios, it was possible to identify the last one as the driving one. Then, an analysis for each phase was carried out, taking into account the power request from all the subsystems.
The optical parameters are selected by using many combinations of different coating materials. In the end, to insulate the components that require higher operative temperatures, such as the tanks, 20 and 25 layers of Aluminized mylar are used on the external side, for ARGO and IASON respectively. On the internal side, a layer of Kapton double Goldized is used. For the other surfaces, a 2 mm layer of grey paint and a 1mm layer of white paint are used on the external and internal surfaces respectively.
A relevant tuning parameter, used to satisfy both hot and cold conditions, is the tilting angle of the solar panels. As a matter of fact, solar panels are used as radiators to dissipate the heat excess but also as heaters, by converting the power excess into heat using the shunt resistances. This, together with onboard heaters, produces the heat required by the TCS to keep every component and device inside the working temperature range.

11. Conclusions

As a conclusion of this report the outcomes of the feasibility analyses of the mission are here summarized.
Starting from the main requirements: the effectiveness of the technique is demonstrated with a variation of semi-major axis of 100 m for 3 years of GT. Concerning the characterization of the binary system, this is achieved thanks to both ARGO and IASON observations during the whole mission.
Concerning the gravity tractor technique we can asses that it is useful in the case in which we can predict the possible impact with an asteroid with high time of prediction. Moreover, we want to underline that the time request for that technique strongly depends on the mass involved. Indeed, the higher is the mass of the spacecraft for a given asteroid mass the less will be the time request.

References

[1] B.J. Wall and B.A. Conway, Shape-Based Approach to Low-Thrust Rendezvous Trajectory Design, Journal of Guidance, Control, and Dynamics 32.1 (2009) 95–101.
[2] Wm. Robert Johnston. (162000) 1990 OS, Asteroids with Satellites Database-Johnston's Archive. http://www.johnstonsarchive.net/astro/astmoons/am-162000.html. Sept. 2014.
[3] G. Inalhan, M. Tillerson, J.P. How, Relative Dynamics and Control of Spacecraft Formations in Eccentric Orbits, Journal of Guidance, Control, and Dynamics 25.1 (2002) 48–59.
[4] D.J. Scheeres, Orbital Motion in Strongly Perturbed Environments: Applications to Asteroid, Comet and Planetary Satellite Orbiters, Springer, 2016.
[5] M.C. Jesick, Optimal Lunar Orbit Insertion from a Free Return Trajectory, Diss. (2012).
[6] B. Wie, Dynamics and control of gravity tractor spacecraft for asteroid deflection, Journal of Guidance, Control, and Dynamics 31.5 (2008) 1413–1423.
[7] S. Kulumani, K. Takami, T. Lee, Geometric control for autonomous landing on asteroid Itokawa using

visual localization, arXiv preprint arXiv:1708.09435 (2017).
[8] E.N. Sabudin, R. Omar, H. CKAN, C.K. Melor, Potential field methods and their inherent approaches for path planning, ARPN Journal of Engineering and Applied Sciences (2016) 10801-10805.
[9] F.L. Markley, J.L. Crassidis, Fundamentals of spacecraft attitude determination and control, Springer New York, New York, 2014.
[10] W.J. Larson, J.R. Wertz, Space Mission Analysis and Design, Kluwer Academic Publishers, 1999.
[11] Arianespace, Ariane 6 - User Manual, Ariane Space 1 (2018)
[12] Arianespace, Ariane 5 - User Manual, Ariane Space 5 (2016)
[13] AZUR SPACE, https://satsearch.co/products/azur-space-qj-solar-cell-4g32c-advanced